Molecular dynamics simulations of simple dipolar liquids in spherical cavity: Effects of confinement on structural, dielectric, and dynamical properties

Sanjib Senapati and Amalendu Chandra

Citation: The Journal of Chemical Physics **111**, 1223 (1999); doi: 10.1063/1.479307
View online: http://dx.doi.org/10.1063/1.479307
View Table of Contents: http://scitation.aip.org/content/aip/journal/jcp/111/3?ver=pdfcov
Published by the AIP Publishing

Molecular dynamics simulations of simple dipolar liquids in spherical cavity: Effects of confinement on structural, dielectric, and dynamical properties

Sanjib Senapati and Amalendu Chandra
Department of Chemistry, Indian Institute of Technology, Kanpur, U.P., India 208016

(Received 25 January 1999; accepted 19 April 1999)

The equilibrium and dynamical properties of Stockmayer liquids confined in a spherical cavity are investigated by means of molecular dynamics simulations. The simulations are carried out at varying density and cavity size. Various equilibrium and time dependent quantities such as the spatial and orientational density profiles, dielectric constants, average energies, pressures, components of translational diffusion tensors parallel and perpendicular to the cavity surface, rotational diffusion coefficients and several time correlation functions are calculated and the effects of confinement on the above properties are discussed. The density profiles are found to be highly inhomogeneous near the cavity wall, and the dielectric constant of the liquids in cavity is found to be significantly smaller than that of the bulk phases. The diffusion along the surface normal and also the dipolar orientational relaxation of solvent molecules in cavity are found to slow down because of confinement. The dynamics of solvation of a newly created charge distribution in the cavity is also studied and the results are compared with the dynamics of solvation in bulk solvent. The solvation in the cavity is found to occur at a much slower rate. © *1999 American Institute of Physics.* [S0021-9606(99)70327-2]

I. INTRODUCTION

Understanding the properties of dipolar solvents confined in nanopores or cavities is important in many areas of chemistry, physics and biology. Microporous materials are widely used in separation processes and also in heterogeneous catalysis. Zeolytes, clathrates and fullerenes are molecular sieves having structures with cavities which can hold only a small number of solvent molecules. Nanopores are also present in several classes of membrane transport proteins where water molecules may be found within the pore. Reverse micelles and vesicles also hold a pool of water molecules in confinement. A first step to characterizing the properties of such systems is to examine how solvent molecules behave when they are confined in pores and cavities of molecular dimensions.

In confined systems, the solvent is extremely inhomogeneous and its thermodynamic, dielectric and dynamical properties can be very different from those in the bulk.[1] For example, the confinement can change the dielectric constant of the solvent in the pore or cavity which, in turn, can influence the electrostatic field within the pore and also the dynamic properties. There have been numerous studies, both experimental and computational, on the properties of water in confinement. Experimental studies of water pool confined in reverse micelles and biological pores have revealed a decrease of dielectric constant[2,3] and a dramatic slowing down of the rate of relaxation of water molecules.[4–10] Similar slowing down of relaxation dynamics has also been observed for solvents in cyclodextrin cavity.[11,12] Molecular dynamics simulations of water in smooth hydrophobic pockets and channels[13–16] have indicated that water molecules confined in such environments exhibit a greater degree of order than in the bulk solvent with the formation of molecular layers near the cavity surface. The diffusional properties of water have also been found to be perturbed due to confinement. Molecular dynamics simulations have also been employed to investigate more realistic biological pores.[17–23] Most of these studies attempt to include the specific structure of the pore or channel concerned which makes their analysis quite complicated and system specific. Also, all the above studies of liquid-filled pores and cavities considered water as the solvent. Water is a very complicated liquid because of its hydrogen bonded network. Our aim of the present work is to take a simple model as a reference system for dipolar liquids in cavity and to study its equilibrium and dynamical properties in a detailed manner. From a theoretical point of view, Stockmayer liquids in a smooth spherical cavity appear to be simple model systems for learning about the effects of confinement on properties of dipolar liquids. This simple model will help us to investigate the modifications of the solvent properties which arise from confinement alone and not from any specific solvent-wall interactions.

In this work, we present detailed molecular dynamics simulations of Stockmayer liquids[24] confined in smooth spherical cavity. The simulations are carried out at varying density and cavity size. We have also simulated the corresponding bulk solvent so that the behavior of confined systems can be compared with that of the bulk. The properties of the confined and bulk dipolar molecules are calculated in terms of several equilibrium and time dependent quantities such as the spatial and orientational density profiles, dielectric constants, average energies, pressures, components of translational diffusion tensors parallel and perpendicular to the cavity surface, rotational diffusion coefficients and vari-

ous time correlation functions. The density profiles are found to be highly inhomogeneous near the cavity wall, and the dielectric constant of the liquids in cavity is found to be significantly smaller than that of the bulk phases. The diffusion along the surface normal and also the dipolar orientational relaxation of solvent molecules in the cavity are found to slow down because of confinement.

We have also studied the dynamics of solvent relaxation around a newly created charge distribution in a cavity. Solvation dynamics in bulk solvents has been studied for over 20 years and much of the work has been described in recent reviews.[25–30] These studies have provided valuable information about molecular relaxation in dipolar liquids. Now it is known that for most solvents the solvation occurs in two phases. The first one is a very fast nondiffusive inertial relaxation which occurs in subpicosecond time scale and which accounts for major part of solvation. The second one involves the diffusive motion of solvent molecules which occurs on the time scale of several picoseconds. Recent studies have also investigated solvation dynamics in confined liquids. These latter studies have revealed a much slower rate of solvation in confined medium as compared to that in bulk solvents. Clearly, computer simulations can play an important role in understanding the factors that influence the time scales of molecular processes involved in solvation in confined medium, like in a cavity. It is found that even for solvation in a cavity the relaxation occurs in two phases: a fast inertial response which is followed by a slow diffusive or reorganizational motion. This biphasic relaxation appears to be a general feature of solvation dynamics. For cavity solvation, however, the relaxation times are very different. Especially, the relaxation time of the long-time reorganization appears to be an order of magnitude slower than the corresponding relaxation time of bulk solvation. This slowing down can be primarily attributed to the orientational constraint imposed by the cavity walls, density inhomogeneity and the reduction of dielectric constant of the medium. Of course, all of these effects are interrelated.

The rest of the paper is organized as follows. In Sec. II, we describe the basic model and the simulation details. The results of structural and dielectric properties are described in Sec. III. In Sec. IV, we describe the dynamical properties including solvation dynamics. Our conclusions are summarized in Sec. V.

II. THE MODEL AND SIMULATION DETAILS

We have carried out molecular dynamics simulations of five different systems consisting of dipolar liquids of varying density and confinement. For three of the above systems, the dipolar solvents are confined in spherical cavities of varying size. The remaining two systems consist of bulk solvents. The solvent molecules interact with each other through a spherically symmetric short-range Lennard-Jones potential and an anisotropic long-range electrostatic potential. For confined systems, they also interact with the cavity surface so that the total configurational energy of a cavity system can be expressed in the form

$$U=\frac{1}{2}\sum_{i,j} u_{\mathrm{LJ}}(r_{ij})-\frac{1}{2}\sum_{i=1}^{N}\mu_i\cdot E_i+\sum_{i=1}^{N} u_{ws}(r_i), \tag{1}$$

where N is the total number of solvent molecules, r_{ij} is the distance between molecules i and j and E_i is the electric field at molecule i due to all other dipoles in the system. μ_i is the dipole vector (of magnitude μ) of the ith molecule. $u_{\mathrm{LJ}}(r_{ij})$ is the spherically symmetric Lennard-Jones interaction potential given by

$$u_{\mathrm{LJ}}(r_{ij})=4\epsilon_s[(\sigma_s/r_{ij})^{12}-(\sigma_s/r_{ij})^{6}], \tag{2}$$

where σ_s and ϵ_s are, respectively, the Lennard-Jones diameter and well-depth parameter of solvent molecules. The first two terms of Eq. (1) constitute the so-called Stockmayer potential. The third term in Eq. (1) arises from the interaction of solvent molecules with the cavity wall. We assume that the cavity wall is located at a distance r_0 from the center of the spherical cavity. Following Zhang *et al.*, we describe the interaction of a solvent molecule with the cavity wall by a 9-3 Lennard-Jones potential of the following form:[15]

$$u_{ws}(r)=\frac{3^{3/2}\epsilon_{ws}}{2}[(\sigma_{ws}/r)^{9}-(\sigma_{ws}/r)^{3}], \tag{3}$$

where $r=|r_0-r_i|$, r_i is the distance of the solvent molecule from the center of cavity and ϵ_{ws} and σ_{ws} are the 9-3 Lennard-Jones well-depth parameter and diameter which characterize the wall-solvent interaction. The force on particle i caused by its interaction with the cavity wall is given by

$$\mathbf{F}_w(\mathbf{r})=-\left[\frac{3^{7/2}\epsilon_{ws}\sigma_{ws}^{9}\mathbf{r}_i}{2r_i r^{10}}-\frac{3^{5/2}\epsilon_{ws}\sigma_{ws}^{3}\mathbf{r}_i}{2r_i r^{4}}\right], \tag{4}$$

where $\mathbf{r}_i$ denotes the position of the ith particle in a coordinate frame whose center is located at the center of the cavity. It is clear from the above expression that the wall potential gives rise to a discontinous force at the center of the cavity. However, for the cavity systems considered in the present study, the wall forces are so small near the cavity center that the above discontinuity is immaterial. We also note that the cavity wall as described by Eq. (3) may appear to be hydrophobic at first sight because there are no attractive electrostatic interactions between the cavity surface and the solvent molecules. However, the interior of a spherically symmetric charge distribution has no electric field. Thus, the properties and the simulations would be identical if the cavity wall contained a uniform charge as there is no electric field inside a charged sphere. Therefore, no distinction could be made between a hydrophobic and a hydrophilic cavity in the present conditions.

The systems studied here can be specified by the reduced parameters: the reduced average density $\rho^*=\rho\sigma_s^3$, the reduced dipole moment of a solvent molecule $\mu^*=\sqrt{\mu^2/\epsilon_s\sigma_s^3}$, the reduced moment of inertia $I^*=I/m\sigma_s^2$, the reduced temperature $T^*=k_BT/\epsilon_s$ where k_B is Boltzmann constant and the reduced wall-solvent interaction parameters $\epsilon_{ws}^*=\epsilon_{ws}/\epsilon_s$ and $\sigma_{ws}^*=\sigma_{ws}/\sigma_s$. For all systems we have taken $\mu^*=1.8$, $I^*=0.025$ and $T^*=1.35$. The values of wall-solvent interaction parameters are: $\epsilon_{ws}^*=3.0$ and σ_{ws}^*

TABLE I. Values of different parameters

System	Geometry	Cavity diameter	Density ($\rho\sigma_s^3$)	Time steps
1	cavity	$6\sigma_s$	0.7	4 000 000
2	cavity	$8\sigma_s$	0.7	2 000 000
3	bulk	⋯	0.7	200 000
4	cavity	$6\sigma_s$	0.8	2 500 000
5	bulk	⋯	0.8	200 000

$=0.8$. Systems 1–3 are simulated at an average density of $\rho^*=0.7$ and systems 4–5 are at $\rho^*=0.8$. For bulk systems (systems 3 and 5), simulations are carried out in cubic boxes, the length (L) of which depends on the average density of the system. For system 3, $L=7.15\sigma_s$ and it is $6.84\sigma_s$ for system 5. For these bulk systems, periodic boundary conditions are employed in all directions, minimum image convention is used for the short-range interaction and the Ewald summation method is employed for the long-range dipole–dipole interactions.[31] The Ewald parameters employed are $\alpha/L=6.4$, a reciprocal space cutoff of $15\sigma_s^{-1}$ and $\epsilon'=\infty$.

For the cavity systems, the initial configuration is generated by the bulk simulations. The solvent molecules in a sphere with radius $(r_0-\sigma_{ws})$ are selected from the bulk and are put into the confining spherical surface located at r_0. This corresponds to having 80 molecules for system 1, 188 molecules for system 2 and 90 molecules for system 4. The effective radius R_c of a cavity is defined to be the radial distance from the center where the wall-solvent interaction becomes zero. It is clear from Eq. (3) that $R_c=r_0-\sigma_{ws}$. The MD simulations were carried at constant temperature employing the leap-frog algorithm[32] with a reduced time step $\Delta t^*=\Delta t(\epsilon_s/m\sigma_s^2)^{1/2}=0.0025$. The quaternion formulation was employed for the rotational motion.[32]

The bulk systems were equilibrated for 50 000 time steps and the production runs were continued for 200 000 time steps. The cavity systems were equilibrated for at least 500 000 steps and the production runs were continued for at least 2 000 000 steps. The convergence was found to be much faster for the bulk systems than the cavity systems. The values of the different parameters and the simulation run periods of the five systems are summarized in Table I. The results of the various equlibrium and dynamical properties of the cavity and bulk systems are presented in the following sections.

III. STRUCTURAL AND DIELECTRIC PROPERTIES

We have examined the number density and orientational structure of dipolar molecules next to the cavity wall. The number densities are calculated by computing the average number of molecules in spherical shells of thickness $\Delta r=0.02\sigma_s$, lying at various distances from the center of the cavity. The effects of cavity surface on the orientational structure of different species are determined by calculating the wall-solvent correlation function $g_{ws}(r,\theta)$, where θ is the angle between the dipole vector of a molecule and the surface normal. For convenience, we expand $g_{ws}(r,\theta)$ in the basis set of Legendre polynomials as follows:

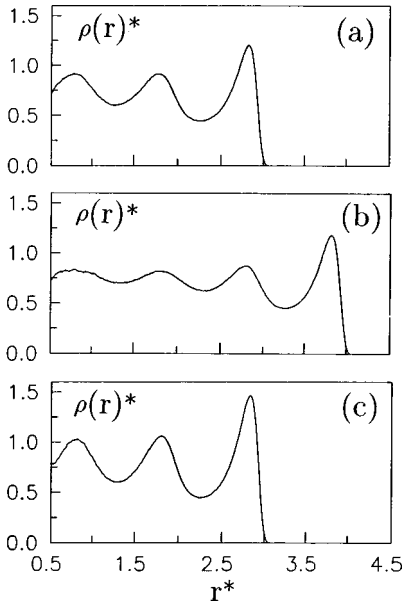

FIG. 1. The position dependence of inhomogeneous number density for the cavity systems (a) system 1, (b) system 2 and (c) system 4. $\rho(r)^*$ is the number density multiplied by σ_s^3 and the reduced distance $r^*=r/\sigma_s$.

$$g_{ws}(r,\theta)=\sum_l (-1)^l g_{ws}^{0ll}(r)P_l(\cos\theta), \tag{5}$$

where $P_l(\cos\theta)$ is the Legendre polynomial of order l. Clearly, $\rho g_{ws}^{000}(r)$ gives the number density of the solvent next to the cavity wall. $g_{ws}^{0ll}(r)$ for $l\neq 0$ gives information about the orientational structure of dipolar molecules near the cavity wall. For the present model, $g_{ws}^{011}(r)$ is zero and the most important orientational term is $g_{ws}^{022}(r)$. We note that a positive value of $g_{ws}^{022}(r)$ implies that the solvent molecules prefer to align perpendicular to the surface and are negative when molecules are aligned parallel to the surface.

In Fig. 1 we have shown the number density $\rho(r)$ as a function of distance from the cavity wall. The results are shown for all cavity systems of varying size and solvent density. The density profiles are seen to be highly nonuniform near the cavity wall. The layering of solvent molecules in the cavity appears to increase with the increase of solvent density. In Fig. 2, we have shown the results of the orientational structure. $g_{ws}^{022}(r)$ is negative near the surfaces which implies that the molecules are aligned parallel to the surface in the vicinity of the wall. This orientational ordering near the cavity wall is similar to those found earlier for planar walls[33,34] and it appears to influence the average energies of the systems as can be seen from Table II. In this table, we have included the average solvent–solvent, wall-solvent interaction energies and also the pressures for all systems considered in this study. The energies of the bulk systems are calculated by using the Ewald summation method for the long-range dipole–dipole interactions. The pressures (P) are calculated in the usual way from the virial.[32] The Lennard-Jones part (U_{LJ}) of the average solvent-solvent interaction energy per molecule is found to be smaller and the dipolar part (U_{dd}) is found to be larger in magnitude for the cavity systems than the corresponding values for the bulk systems.

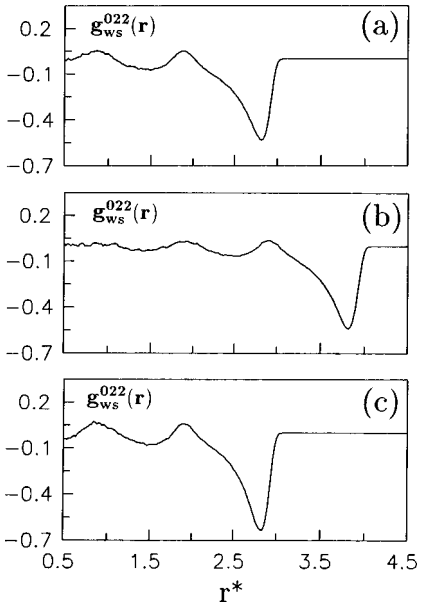

FIG. 2. The position dependence of the inhomogeneous orientational structure $g_{ws}^{022}(r)$. The different curves are as in Fig. 1.

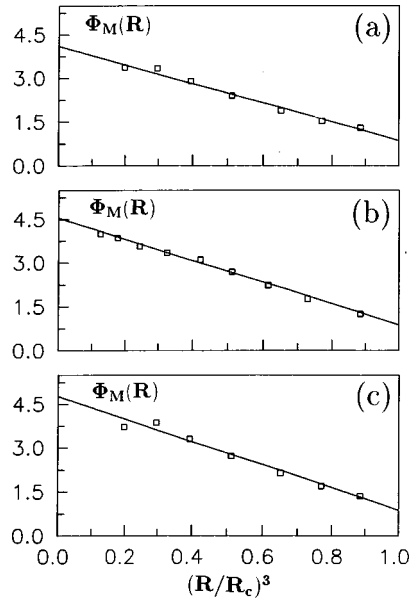

FIG. 3. The value of $\Phi_M(R)$ for different values of R for (a) system 1, (b) system 2 and (c) system 4. The squares represent the simulation results and the solid lines represent the theoretical predictions given by Eq. (6) for (a) $\epsilon=19$, (b) $\epsilon=21$ and for (c) $\epsilon=22$.

This can be attributed to the strong inhomogeneity and the orientational ordering of solvent molecules near the cavity surfaces. The average wall-solvent interation energy (U_{ws}) per molecule is found to be larger in magnitude for the smaller cavity with the same average density. The pressure of the cavity systems is found to be higher than the bulk systems due to confinement.

We now discuss the dielectric propeties of the bulk and cavity systems. We have calculated the dielectric constant of the solvents in cavity by using a formulation first derived by Berendsen[35] and subsequently used by others[36–38] in different connections. In this formulation, the dielectric constant of a solvent-filled spherical cavity of radius R_c is calculated by calculating the mean square moment fluctuation $\langle M^2\rangle_R$ within a sphere of radius R, smaller than the cavity radius R_c and concentric with it. Since interactions among all dipolar molecules are included during simulations, the mean square moment fluctuation in a smaller sphere of radius R includes the effects of the reaction field due to the shell for which $R<r<R_c$ and, as a result, $\langle M^2\rangle_R$ depends on the dielectric constant and also on the ratio R/R_c. Following the method of Frohlich,[39] Berendsen showed that when the medium surrounding the solvent sphere is nonpolarizable, the mean square moment fluctuation $\langle M^2\rangle_R$ is related to the dielectric constant ϵ of the solvent in cavity by the following relation:

$$\Phi_M(R)=\frac{(\epsilon-1)}{9\epsilon(\epsilon+2)}\left[(\epsilon+2)(2\epsilon+1)-2(\epsilon-1)^2\left(\frac{R}{R_c}\right)^3\right], \tag{6}$$

where $\Phi_M(R)=\langle M^2\rangle_R/3k_BTR^3$. The above equation has been used by Adams and McDonald[36] for polar lattices, by Powles *et al.* for liquid drops[37] and its two-dimensional generalization has also been used by Bossis *et al.*[38] A generalization of the above equation is also available for cases where the dielectric constant of the surrounding medium (the cavity wall in the present context) is not unity and is polarizable.[36] Since the cavity wall is nonpolarizable for the systems considered in this study, we have used Eq. (6) to calculate the dielectric constant of the solvent in the cavity.

We have calculated the quantity $\Phi_M(R)$ for various different values of R through simulations and have compared the simulation values with the theoretically predicted values as given by Eq. (6). The results are summarized in Fig. 3. The simulation results agree quite well with the predicted linear variation of $\Phi_M(R)$ with R. The small fluctuations of the simulation data from the linear behavior can be attributed to the smaller number of particles in spherical regions of smaller radii and also to the inhomogeneity of the medium inside the cavity. From the least-square fitting of the simulation data to the predictions of Eq. (6), one can infer that the value of ϵ is 19 for system 1, 21 for system 2 and it is 22 for system 4. For bulk systems (systems 3 and 5), we have used the well-known relation between the total mean square moment fluctuation and the dielectric constant for the Ewald boundary condition. The bulk simulations provide the following values: $\epsilon=31$ for system 3 and it is 47 for system 5.

TABLE II. The average solvent–solvent and wall-solvent interaction energies, pressures and the dielectric constants of various systems studied in this work. $U^*=U/N\epsilon_s$ and $P^*=P\sigma_s^3/\epsilon_s$ where N is the number of molecules in a simulation system.

System	U_{LJ}^*	U_{dd}^*	U_{ws}^*	P^*	ϵ
1	−2.62	−6.58	−1.59	0.30	19
2	−3.03	−5.19	−1.30	0.07	21
3	−4.34	−4.58	⋯	−0.92	31
4	−2.84	−6.84	−1.63	0.65	22
5	−4.88	−4.96	⋯	−0.23	47

These values of the dielectric constants for systems 1–5 are included in Table II. Clearly, the confinement leads to a noticeable lowering of the dielectric constant of the solvents investigated in this study. In this context we note that such reduction of the dielectric constant of a medium in confinement has also been reported earlier in experimental and simulation studies of water in reverse micelles[2,3] and in protein environments.[23] In such cases, the reduction of the dielectric constant was analyzed primarily in terms of electrostatic interaction of the water molecules with charged surfaces. Such interactions result in rotationally bound molecules which are not available for response to an external field. In the present systems, there is no electrostatic interaction between a solvent molecule and the cavity surface and, therefore, reduction of the dielectric constant observed in the present study is purely a result of confinement.

IV. DYNAMIC PROPERTIES

We present various dynamical properties of the solvent-filled cavities that we have investigated in the present work. The major objective has been to study the perturbations of the solvent dynamics induced by the confinement of a cavity. We have calculated the velocity and angular velocity autocorrelation functions, translational and rotational diffusion coefficients and also the relaxation of dipolar orientational correlation functions. The above dynamical quantities are calculated as functions of cavity size and density. We denote the velocity of a dipolar molecule by $v(t)$ and its normalized velocity autocorrelation function (VAF) $C_v(t)$ is defined by[40]

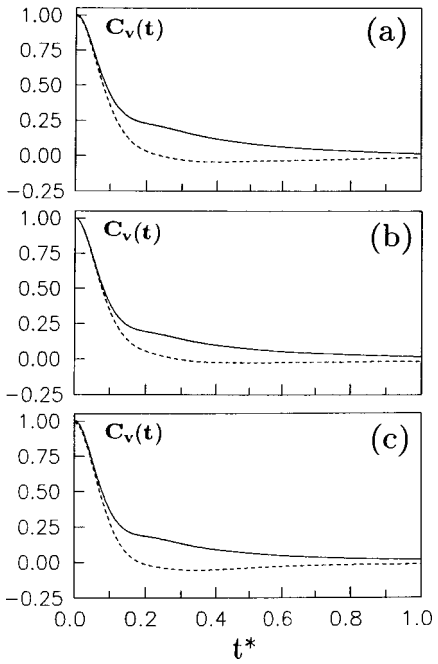

FIG. 4. The time dependence of the velocity–velocity autocorrelation functions for (a) system 1, (b) system 2, (c) system 4. The solid and dashed curves show the relaxation of the parallel ($\|$) and perpendicular ($\perp$) components of $C_v(t)$, respectively.

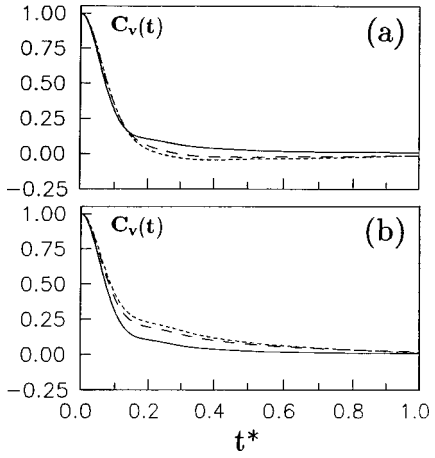

FIG. 5. The comparison of the relaxation of velocity autocorrelation functions in cavity (systems 1–2) and in the bulk phase (systems 3): (a) perpendicular ($\perp$) (b) parallel ($\|$) components of $C_v(t)$. The dotted, dashed and the solid curves are for systems 1, 2 and 3, respectively.

$$C_v(t)=\frac{\langle v(t)\cdot v(0)\rangle}{\langle v(0)^2\rangle}, \tag{7}$$

where $\langle\cdots\rangle$ represents an equilibrium ensemble average. Because of the presence of the cavity wall, the diffusion in directions parallel and perpendicular to the surface tangent can be different. This is illustrated in Figs. 4 and 5 where we have shown the decay of the parallel ($\|$) and perpendicular ($\perp$) components of velocity–velocity autocorrelation functions for the dipolar molecules in cavity. In all the figures, the two velocity components are seen to decay differently. Clearly, diffusion along the parallel direction is expected to be quite different from that in the perpendicular direction. The translational diffusion coefficient D can be calculated from the VAF by using the following relation:[40]

$$D=\frac{k_BT}{m}\int_0^\infty C_v(t)dt. \tag{8}$$

The parallel and perpendicular components of the diffusion coefficient can be calculated by integrating the parallel and perpendicular (to the surface tangent) components of the VAF and the results are shown in Table III. We note that there are a few problems associated with the meaning of diffusion in a confined inhomogeneous environment. One is that there is a limit on the mean square displacement due to confinement. As a result, the values of diffusion coefficients depend on the time scale of evaluation of the relevant correlation functions. This problem can be overcome by calculat-

TABLE III. Translational diffusion coefficients of dipolar molecules of various systems studied in this work. The quoted errors are estimated standard deviations. $D^*=D(m/\epsilon_s\sigma_s^2)^{1/2}$.

System	$D_\perp^*$	$D_\|^*$	D^*
1	0.083±0.002	0.224±0.006	0.177±0.004
2	0.090±0.003	0.214±0.006	0.173±0.004
3	0.143±0.004	0.143±0.004	0.143±0.004
4	0.066±0.002	0.184±0.002	0.145±0.003
5	0.096±0.003	0.096±0.003	0.096±0.003

TABLE IV. Rotational diffusion coefficients and orientational relaxation time of dipolar molecules of various systems studied in this work. The quoted errors are estimated standard deviations. $\Theta^* = \Theta(m\sigma_s^2/\epsilon_s)^{1/2}$ and $\tau_1^* = \tau_1(m\sigma_s^2/\epsilon_s)^{1/2}$.

Quantity	System 1	System 2	System 3	System 4	System 5
Θ^*	3.21±0.036	3.04±0.026	2.76±0.03	3.00±0.015	2.65±0.03
τ_1^*	0.30	0.29	0.25	0.31	0.26

ing the correlation functions over a time before the effects of the walls become apparent. In the present study, the diffusion coefficients are calculated by integrating the VAF over a time of $t^*=1.0$ where t^* is the reduced time as defined in Sec. II. It may be noted that the velocity autocorrelation functions have essentially decayed to zero in the above time scale. Also the root mean square displacement of molecules over the above time scale has been found to be much smaller than the cavity diameters. The other problem is that a molecule diffusing in a region of varying density experiences a mean force depending on its position and one would expect the diffusion coefficient to vary with the local density. In the present work, the velocity autocorrelation functions are calculated by averaging over all molecules in a system and, therefore, the diffusion coefficients reported in Table III should be considered as effective diffusion coefficients. The diffusion coefficients in the corresponding bulk phases (systems 3 and 5) are also included in the table for comparison. Note that in the bulk phase, the diffusion is isotropic so that $D_\parallel = D_\perp$. The error bars included in the table are the standard deviations which are determined by dividing the total run period into blocks of 100 000 time steps (25 000 time steps in the case of bulk systems) and treating the block averages as independent estimates of the time correlation functions and diffusion coefficients. It is seen that the diffusion along the perpendicular direction ($D_\perp$) is considerably slower than diffusion in the bulk phases. The wall-solvent interaction inhibits motion along the perpendicular direction. The values of $D_\parallel$ show an enhanced diffusion along the parallel direction. The force from the cavity wall acts only along r-direction (i.e., perpendicular) and the solvent molecules in the cavity feel a less effective friction for motion along the parallel direction, especially those near the cavity wall since there are no solvent molecules on the other side of the wall and this leads to increased values of $D_\parallel$.

In Table IV, we have shown the rotational diffusion coefficients of dipolar molecules in the cavity systems and in bulk phases. Here again, the rotational diffusion coefficients are calculated by integrating the angular velocity autocorrelation functions over a time of $t^*=1$. The rotational diffusion coefficients in the cavity are found to be higher than the corresponding bulk values. Near the cavity wall, a molecule is surrounded by less molecules because of the presence of the solid surface, and as a result, the magnitude of torque that is exerted on the molecule is less than that on a bulk molecule. This reduced torque tends to accelerate whereas orientational constraint tends to slow down the rotational motion of interfacial dipolar molecules. For the present systems, the orientational constraint is much less and the effects of reduced torque become important and as a result we observe an enhanced rotational diffusion in the cavity.

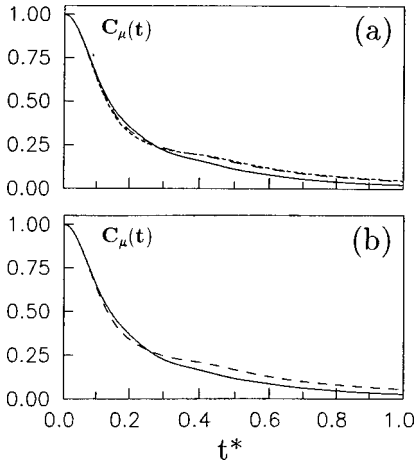

FIG. 6. The time dependence of the dipolar orientational correlation functions in cavity and in the bulk phase: (a) the dotted, dashed and the solid curves are for systems 1, 2 and 3, respectively. (b) The dashed and solid curves are for systems 4 and 5, respectively.

We next discuss the effects of confinement on the relaxation of the dipolar orientational correlation function, $C^\mu(t)$, defined by

$$C^\mu(t) = \langle \mu(t)\cdot\mu(0)\rangle / \langle \mu(0)\cdot\mu(0)\rangle, \tag{9}$$

where $\mu(t)$ is the dipole vector of a molecule. The results of $C^\mu(t)$ for the cavity systems are shown in Fig. 6. Again, the results of the bulk phases are also included for comparison. The dipolar relaxation in the cavity is seen to occur at a slower rate than that of bulk molecules. To quantify the slowing down of the dipolar orientational relaxation, we have fitted the long-time decay of $C^\mu(t)$ to an exponential function e^{-t/τ_1} where τ_1 is the single particle orientational relaxation time. The values of τ_1 for all the systems are included in Table IV. The orientational relaxation in cavity is found to slow down by about 20% compared to the rate of relaxation in the corresponding bulk phases.

We next report the results of the dynamics of solvation of a newly created charge distribution in the cavity. Such studies can provide useful information about the dynamic response of a confined dipolar medium. We consider a neutral Lennard-Jones solute located near the cavity wall. After equilibration, the neutral solute is suddenly charged to an ion. The reduced charge ($q^* = \sqrt{q^2/\epsilon_s\sigma_s}$) of the solute ion is 16. The subsequent time dependence of the solute-solvent electrostatic energy, $U_{ID}(t)$, is recorded. The time dependence of this interaction energy reflects how fast the solvent molecules in the cavity can adjust (or respond) to the newly created nonequilibrium environment. The experimental results of solvation dynamics are usually analyzed in terms of the normalized solvation function defined by

$$S(t) = \frac{U_{ID}(t) - U_{ID}(t=\infty)}{U_{ID}(t=0) - U_{ID}(t=\infty)}. \tag{10}$$

As solvation progresses, $S(t)$ decays from 1 to 0. $S(t)$ is directly related to the experimentally measured solvation dynamics through the time dependent fluorescence Stokes shift.

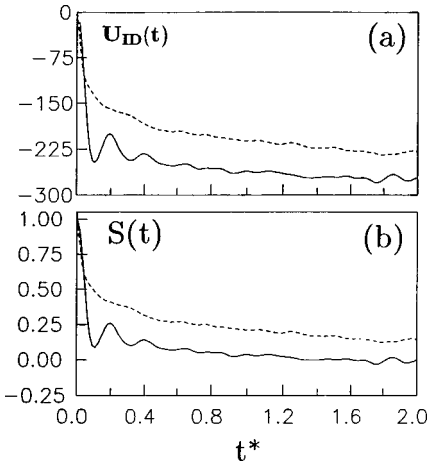

FIG. 7. The time dependence of (a) solute-solvent interaction energy $U_{ID}(t)$ (expressed in units of ϵ_s) and (b) normalized solvation function $S(t)$ for system 1. The dotted and the solid curves represent the results of dynamics of solvation of a charged solute located at the surface in the cavity and in bulk, respectively. The equilibrium values of $U_{ID}(t)$ for solvation in cavity and in bulk are $-264.2\epsilon_s$ and $-278.4\epsilon_s$, respectively.

In the present work, we have focused on the following issues: How does the confinement of the dipolar liquid affect the dynamics of solvation and to what extent the solvation dynamics in cavity is different from that in a bulk solvent? We have addressed the above issues by calculating the time dependence of $U_{ID}(t)$ and $S(t)$ for system 1 keeping the solute fixed near the cavity surface. We have also calculated the dynamics of solvation in the corresponding bulk system (system 3). All results are obtained by averaging over a minimum of 40 independent nonequilibrium trajectories.

In Fig. 7(a), we have shown the results of $U_{ID}(t)$ for solvation in system 1. The results for the bulk liquid are also shown for comparison. The solvation energy of the solute at the cavity surface is found to be smaller than that of the solute in bulk solvent. For the solute at the cavity surface, the surrounding solvation shell is not spherical (or complete) because of the presence of the cavity surface at one side of the solute and this leads to a decrease of solvation energy. In Fig. 7(b), we have plotted the time dependence of the normalized solvation function $S(t)$ for system 1 and for the corresponding bulk phase. The solvation in the cavity is found to be much slower than bulk solvation. The contribution of the ultrafast inertial relaxation at short times is diminished for cavity solvation. The short-time decay of $S(t)$ can be described quite well by a Gaussian function of the form e^{-t^2/τ_g^2} and the long-time decay is fitted to an exponential function of the form e^{-t/τ_e}. A least-square fit to the short-time and long-time parts of $S(t)$ gives the following values: $\tau_g^*=0.11$, $\tau_e^*=1.40$ for solvation in cavity and $\tau_g^*=0.06$, $\tau_e^*=0.28$ for bulk solvation, where τ^* is the reduced (or dimensionless) relaxation time equal to $\tau(m\sigma_s^2/\epsilon_s)^{1/2}$.

V. SUMMARY AND CONCLUSIONS

We have carried out molecular dynamics simulations of dipolar liquids confined in a spherical cavity. Five different systems of varying density and cavity size are investigated. Various structural, dielectric and dynamical properties of the confined solvent are calculated and compared with the corresponding quantities in the bulk. It is found that the properties of the confined solvent can be quite different from those of the bulk phases.

The density profiles in the cavity are found to be highly nonuniform. Pronounced orientational order is found for the dipolar molecules which are seen to align parallel to the cavity wall. This orientational ordering leads to a lowering of the dielectric constant of the solvent in a cavity as compared to its bulk value. The translational motion of the confined molecules is calculated in directions perpendicular and parallel to the surface tangent. It is found that the perpendicular diffusion is hindered and the lateral diffusion is enhanced compared to diffusion in the bulk phases. The dipolar orientational relaxation in a cavity is also found to be slower than that in the bulk phases and the extent of slowing down is found to increase with decreasing cavity size. Studies of solvation dynamics reveal a significant slowing down of the rate of solvation in a cavity than that in the bulk solvent. The slowing down can be attributed primarily to the slower orientational relaxation of solvent molecules in the cavity. To the best of our knowledge, such slowing down of solvation in a cavity is reported here for the first time by means of molecular dynamics simulations.

ACKNOWLEDGMENT

The financial support of the Council of Scientific and Industrial Research (CSIR), Government of India, is gratefully acknowledged.

[1] J. N. Israelachvili, *Intermolecular and Surface Forces* (Academic, New York, 1992).
[2] M. Belletete, M. Lachapelle, and G. Durocher, J. Phys. Chem. **94**, 5337 (1990).
[3] J. Guha Ray and P. K. Sengupta, Chem. Phys. Lett. **230**, 75 (1994).
[4] S. Mashimo, S. Kuwabara, S. Yagihara, and K. Higasi, J. Phys. Chem. **91**, 6337 (1987).
[5] M. Fukazaki, N. Miura, N. Shiyasilki, D. Kunita, S. Shioya, M. Haida, and S. Mashimo, J. Phys. Chem. **99**, 431 (1995).
[6] P. O. Quist and B. Halle, J. Chem. Soc., Faraday Trans. 1 **84**, 1033 (1988).
[7] D. Brown and J. H. R. Clarke, J. Phys. Chem. **92**, 2881 (1988).
[8] R. E. Riter, D. M. Willard, and N. E. Levinger, J. Phys. Chem. B **102**, 2705 (1998).
[9] N. Sarkar, K. Das, A. Dutta, S. Das, and K. Bhattacharya, J. Phys. Chem. **100**, 10523 (1996).
[10] A. Dutta, D. Mandal, S. K. Pal, and K. Bhattacharya, J. Phys. Chem. B **101**, 10221 (1997).
[11] S. Vajda, R. Jimenez, S. Rosenthal, V. Fidler, G. R. Fleming, and E. W. Castner, Jr., J. Chem. Soc., Faraday Trans. **91**, 867 (1995).
[12] N. Nandi and B. Bagchi, Indian J. Chem. **34A**, 845 (1995); J. Phys. Chem. **100**, 13914 (1996).
[13] A. C. Belch and M. Berkowitz, Chem. Phys. Lett. **113**, 278 (1985).
[14] M. S. P. Sanson, I. D. Kerr, J. Breed, and R. Sankararamakrishnan, Biophys. J. **70**, 693 (1996).
[15] L. Zhang, H. T. Davis, D. M. Kroll, and H. S. White, J. Phys. Chem. **99**, 2878 (1995).
[16] R. M. Lynden-Bell and J. C. Rasaiah, J. Chem. Phys. **105**, 9266 (1996).
[17] S. W. Chiu, E. Jakobsson, S. Subramanian, and J. A. McCammon, Biophys. J. **60**, 273 (1991).
[18] D. H. J. McKay, P. H. Berens, K. R. Wilson, and A. J. Hagler, Biophys. J. **46**, 229 (1984).
[19] P. C. Jordan, J. Phys. Chem. **91**, 6582 (1987); Biophys. J. **58**, 1133 (1990).
[20] J. Aquist and A. Warshel, J. Chem. Phys. **56**, 171 (1989).
[21] B. Roux and K. Karplus, Annu. Rev. Biophys. Biomol. Struct. **23**, 731 (1994).

[22] J. Breed, R. Sankararamakrishnan, I. D. Kerr, and M. S. P. Sansom, Biophys. J. **70**, 1643 (1996).
[23] M. A. Young, B. Jayaram, and D. L. Beveridge, J. Phys. Chem. B **102**, 7666 (1998).
[24] W. H. Stockmayer, J. Chem. Phys. **9**, 398 (1941).
[25] B. Bagchi, Annu. Rev. Phys. Chem. **40**, 115 (1989).
[26] P. Barbara and W. Jarzeba, Adv. Photochem. **15**, 1 (1990).
[27] G. R. Fleming and P. G. Wolynes, Phys. Today **43**, 36 (1990).
[28] B. Bagchi and A. Chandra, Adv. Chem. Phys. **80**, 1 (1991).
[29] M. Maroncelli, J. Mol. Liq. **57**, 1 (1993).
[30] R. M. Stratt, Acc. Chem. Res. **28**, 201 (1995).
[31] S. W. de Leeuw, J. W. Perram, and E. R. Smith, Annu. Rev. Phys. Chem. **37**, 245 (1986); Proc. R. Soc. London, Ser. A **373**, 27 (1980); **388**, 177 (1983).
[32] M. P. Allen and D. J. Tildesley, *Computer Simulation of Liquids* (Clarendon, London, 1987).
[33] S. Senapati and A. Chandra, Chem. Phys. **231**, 65 (1998); J. Mol. Struct.: THEOCHEM **455**, 1 (1998).
[34] S. Senapati and A. Chandra, Chem. Phys. **242**, 353 (1999).
[35] D. J. Berendsen, ''Molecular Dynamics and Monte Carlo Calculations on Water,'' CECAM Report (1972).
[36] D. J. Adams and I. R. McDonald, Mol. Phys. **32**, 931 (1976).
[37] J. G. Powles, R. F. Fowler, and W. A. B. Evans, Chem. Phys. Lett. **107**, 280 (1984).
[38] I. G. Bossis, Mol. Phys. **38**, 2023 (1979).
[39] H. Frohlich, *Theory of Dielectrics* (Clarendon, Oxford, 1949).
[40] J. P. Hansen and I. R. McDonald, *Theory of Simple Liquids* (Academic, London, 1986).